

On the Reliability of Frequency-Domain Features for fNIRS BCIs in the Presence of Pain

A. Subramanian¹, F. Shamsi² and L. Najafizadeh¹

1. Department of Electrical and Computer Engineering, Rutgers University, Piscataway, New Jersey, USA
2. Department of Psychology, Northeastern University, Boston, Massachusetts, USA
{ashwini.subramanian, laleh.najafizadeh}@rutgers.edu, f.shamsi@northeastern.edu

Abstract— In this paper, we study the effects of the presence of pain on the classification accuracy of mental arithmetic tasks in functional near infrared spectroscopy (fNIRS)-based brain computer interfaces (BCIs). fNIRS recordings from prefrontal and motor cortices are obtained during the execution of two mental arithmetic tasks in the presence and absence of external pain stimuli. Various frequency-domain parameters of the fNIRS signals, under pain-free and pain conditions, are extracted for each task and used as features. A support vector machine with a quadratic kernel (QSVM) is used as the classifier. Four scenarios for training and testing the classifier are considered: (1) train and test using pain-free data, (2) train and test using under-pain data, (3) train using pain-free data and test using under-pain data, and (4) train using under-pain data and test using pain-free data. Results show that the classification accuracy of the model trained on pain-free data is significantly reduced when the model is tested on data obtained in the presence of pain. Similarly, the accuracy drops when the model is trained on data obtained in the presence of pain but tested on pain-free data. These results highlight the importance of considering pain-induced changes in cortical activity when developing BCIs for patients in need of them.

I. INTRODUCTION

Functional near infrared spectroscopy (fNIRS) is a non-invasive neuroimaging technique that detects hemodynamic changes in the cerebral cortex in response to external stimuli. In fNIRS, light sources and detectors are placed on the scalp. By measuring changes in the received light intensities at two different wavelengths, changes in the concentrations of oxygenated hemoglobin ($[\Delta HbO_2]$) and deoxygenated hemoglobin ($[\Delta HbR]$), associated with the underlying brain activities, can be estimated using the modified Beer-Lambert's law [1]. Compared to other modalities, fNIRS offers a better temporal resolution than functional magnetic resonance imaging (fMRI), and a better spatial resolution than electroencephalography (EEG) [1].

A brain computer interface (BCI) converts the signals acquired from the brain pertaining to the user's intentions into commands that can be used to control peripheral devices. EEG has been the most commonly-used neuroimaging modality for acquiring signals from the brain in BCIs [2]. Recently, fNIRS, due to its portability and other advantages, has also been emerging as a non-invasive modality in BCIs for acquiring signals from the brain [3]-[9].

A promising application for BCIs is the development of assistive devices for patients with motor and communication disabilities [10]. Patients with motor disabilities may not be able to use their limbs to perform certain tasks. Voice activated assistive devices will not be helpful when the motor disability is accompanied by the absence of communication abilities. However, such patients may still retain their cognitive abilities. For these patients, a BCI can be used to convert the brain signals corresponding to mental processing of a given task into commands for controlling peripheral devices.

Pain is among the secondary conditions that is prevalent in patients with motor or communication disabilities. The pain could be chronic (i.e., it may last for a long duration), or acute (i.e., it has a sudden unpredictable onset with a relatively short duration). The presence of pain is expected to influence cortical activities [11]-[18]. The influence of pain on cortical activity suggests that if the subject does not experience pain during the training process of the BCI, but later experiences pain while using the device for assistive purposes, the device could potentially fail to function as intended. A similar outcome is expected when the patient experiences pain during the training stage of BCI, but does not experience pain during the application stage.

This paper aims to investigate the impact of the presence of pain on the classification accuracy of fNIRS-based BCIs when frequency-domain parameters are used as features. Cortical activities are recorded during two mental arithmetic tasks under two conditions: pain-free and under-pain. Thermal stimulation is used to induce pain of acute nature. A support vector machine classifier with a quadratic kernel (QSVM) is used to classify the two mental arithmetic tasks under four training and testing scenarios. As will be shown, when the classifier is trained using pain-free data and tested using under-pain data, or when it is trained using under-pain data and tested using pain-free data, the classification accuracy significantly drops. Our results suggest that it is essential to consider the presence of pain in developing BCI algorithms for patients.

The remainder of this paper is organized as follows. Experimental procedure and data analysis are described in Sections II and III, respectively. Results and discussions are presented in Section IV, and the conclusions are presented in Section V.

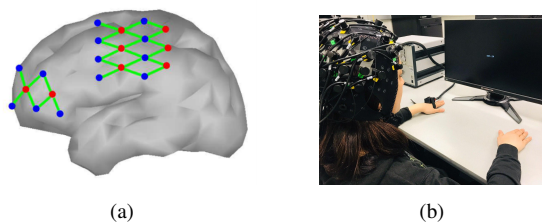


Figure 1. (a): Placement of optodes and channel configuration: red circles indicate light sources, blue circles indicate light detectors and green lines indicate the channels. (b): Experimental setup

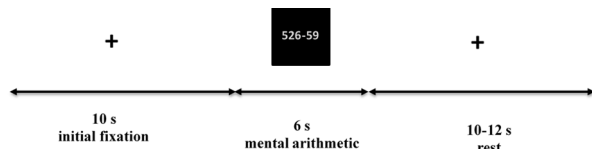


Figure 2. Visual illustration of a single trial

II. EXPERIMENTAL PROCEDURE

Data was collected from three healthy subjects in the NeuroImaging Laboratory at Rutgers University. Written consents approved by the Rutgers' Institutional Review Board (IRB) were obtained from subjects prior to performing the experiments.

fNIRS signals were recorded using NIRx system (NIRScout, NIRx Medical Technologies, LLC) at wavelengths of 760 nm and 830 nm, and at a sampling frequency of 10.41 Hz. 16 sources and 24 detectors were placed over the prefrontal (PF) and the motor cortices, resulting in a total of 50 channels. Figure 1 shows the experimental setup and the location of channels on one side of the brain. The same configuration was used on the other side.

The experiment included 5 pain-free and 5 under-pain blocks that were presented to the subjects in a random order. In each block, subjects were shown a screen where the instruction for executing one of the two considered mental arithmetic tasks was displayed. In one task, the subjects were asked to perform a mental subtraction of two displayed numbers (i.e., subtracting a 2-digit number from a 3-digit number). The other task was a countdown task, during which the subjects were asked to count backward starting from the displayed 2-digit number. Each trial of the experiment consisted of a mental arithmetic task interval lasting 6 seconds, followed by a rest inter-trial interval of 10-12 seconds. Figure 2 visually illustrates the timing of each trial. Each block consisted of 13 trials of each task, resulting in a total of 65 trials per task and per condition (pain-free or under-pain).

For the pain-free block, subjects performed the tasks based on the instruction shown on the screen. For the



Figure 3. Placement of thermode for inducing pain

under-pain blocks, subjects were exposed to thermal pain while they performed the tasks. Pain was induced by applying heat to the dorsum of the left hand via a standard 30×30 thermode from TSA-II from Medoc (see Figure 3). For each subject, temperature points related to pain threshold and tolerance were measured prior to fNIRS recording sessions, using the procedure described in [18]. Briefly, for each subject, the pain threshold was measured by increasing the temperature from the baseline of 32°C at the rate of 1°C/s . The temperature that became painful for the subject was noted as the threshold point. The tolerance temperature was noted as the temperature where the pain became intolerable. For each subject, the mean of the threshold and the tolerance temperature points was considered as the pain temperature, which was applied during fNIRS recording sessions for the under-pain blocks. For pain-free blocks, the temperature of thermode was set to baseline. During the experiment, the position of the thermode was slightly changed on the dorsum to avoid habituation to heat.

III. DATA ANALYSIS

The interval from $[-1-6]$ seconds, where 0 indicates the onset of stimulus, was selected from each trial. Pre-processing of the recorded signals was performed using nirsLAB. Signals were first corrected for drifts and artifacts. Next, a bandpass filter with a passband range of 0.01 to 0.2 Hz was applied to remove the cardiac signal and low-frequency oscillations. Using the modified Beer-Lambert's law [1], the filtered optical intensity signals were converted to $[\Delta HbO_2]$ and $[\Delta HbR]$. For each trial, baseline correction was done by subtracting the average of 1 second of the signal before the onset of the stimulus from the signal. Only $[\Delta HbO_2]$ was used for further analysis, as it is known to have a better signal to noise ratio compared to $[\Delta HbR]$.

Table 1 lists the parameters from the frequency-domain representation of the pre-processed $[\Delta HbO_2]$ signal that were used as features for the classifier in this study. Features were extracted during the $[0-6]$ seconds interval from all the channels. To obtain sufficient number of samples to train the classifier and avoid underfitting, the $[0-6]$ seconds interval was divided into 0.5 second segments. Features were extracted from each segment. This resulted in a total of 12 features from

each 0.5-seconds segment of the considered interval, per channel and per trial. The segments were made non-overlapping to avoid data leakage between the training and testing sets. Extracted features from all trials were split into two randomized groups, one for training (75%) and the other for testing (25%). The training step is representative of the customization step of BCI for the patients and the testing step is representative of the application phase of the BCI.

Table 1. List of frequency-domain features used in this study obtained from discrete Fourier transform (DFT) and power spectral density (PSD)

Feature	Notation
Maximum value of power spectral density	Max PSD
Median value of power spectral density	Med PSD
Variance value of power spectral density	Var PSD
Maximum value of real part of DFT	Max Real{DFT}
Frequency corresponding to Max Real{DFT}	Freq of Max Real{DFT}
Frequency corresponding to maximum value of power	Freq of Max PSD

A support vector machine with a quadratic kernel was used as the classifier. Since the data was not linearly separable, a linear kernel function was not used. No substantial difference in results were observed in using a more complex kernel such as the radial basis function (RBF) that yielded a more complex decision boundary at the cost of increased processing time. For this reason, the QSVM was chosen as a good compromise over the slower RBF kernel. 10-fold cross validation was employed to avoid overfitting the model.

IV. RESULTS

Classification of the two mental arithmetic tasks of subtraction and backward counting were performed under four scenarios. In scenario 1, the SVM classifier was trained and tested using pain-free data. In scenario 2, the classifier was trained using pain-free data but tested using the data obtained in the presence of pain. In scenario 3, the classifier was trained and tested using the data obtained in the presence of pain, and in scenario 4, the classifier was trained using the data obtained in the presence of pain but tested using pain-free data. The results for classification accuracy, averaged across all subjects, are tabulated in Tables 2-5.

Table 2. Classification accuracy results (%) for scenario 1

Features	Scenario 1		
	All	PF	Motor
Max PSD	84.87±2.2	71.08±2.2	83.26±2.1
Med PSD	85.09±2	71.56±1.9	83.91±2.1
Var PSD	76.60±2.6	56.81±4.8	75.60±2.3
Max Real{DFT}	88.65±1.9	72.24±2.2	86.60±2
Freq of Max Real{DFT}	81.47±1.9	63.01±2.3	77.41±1.9
Freq of Max PSD	50.43±2.4	49.36±2.1	49.74±2.2

In scenario 1, not much difference in the $[\Delta HbO_2]$ signals from the training and testing phases is expected, and therefore, a high accuracy is achieved. This scenario resembles cases in which the patient does not experience

pain during both the customization and the application phases. Using features from all 50 channels, the maximum value of the real part of the discrete Fourier transform (DFT) delivers the maximum classification accuracy (88.65%), while the frequency corresponding to the maximum power gives the lowest classification accuracy (see Table 2). The achieved classification accuracy results for this scenario match that of prior work that have used frequency-domain features in their classification algorithms [13].

Table 3. Classification accuracy results (%) for scenario 2

Features	Scenario 2		
	All	PF	Motor
Max PSD	50.72±2.5	54.13±2.4	50.36±2.3
Med PSD	51.09±2.3	54.72±2.3	50.22±2.3
Var PSD	50.46±2.4	51.63±2.7	50.27±2.6
Max Real{DFT}	52.68±2.6	52.4±2.6	52.32±2.6
Freq of Max Real{DFT}	50.51±2.7	51.83±3	50.63±2.4
Freq of Max PSD	50.71±2.2	49.67±2.1	51±2.1

In scenario 2, where the classifier was trained using pain-free data but tested using under-pain data, is akin to the situation where the patient does not experience pain during the customization phase but experiences acute pain during the operating phase of the BCI. The presence of pain is expected to influence cortical brain activities and thus, the $[\Delta HbO_2]$ signals [11]. In this scenario, the average classification accuracy significantly drops to almost the chance level (see Table 3), suggesting the influence of pain on brain activity. The results suggest that a model that is trained on pain-free data will fail to perform in the presence of pain, and the BCI-controlled peripheral device is certain to not perform as intended.

Table 4. Classification accuracy results (%) for scenario 3

Features	Scenario 3		
	All	PF	Motor
Max PSD	85.09±2.3	72.49±2.2	82.75±2.3
Med PSD	85.02±2.2	72.68±2.4	83.07±2.3
Var PSD	76.02±2.3	60.29±3.2	73.69±2.6
Max Real{DFT}	89.91±1.7	73.65±2	87.09±1.9
Freq of Max Real{DFT}	83.14±2.7	65.54±2.3	80.13±1.9
Freq of Max PSD	49.96±2.1	48.80±2	50.82±2.4

Scenario 3 is representative of a case where the patient experiences pain of similar nature during both the customization and the operating phases of the BCI. Once again, the maximum value of the real part of the DFT delivers the maximum classification accuracy (89.91%), while the frequency corresponding to the maximum power gives the lowest classification accuracy result (see Table 4).

Scenario 4 presents a situation where the patient experiences acute pain during the customization phase but does not experience pain during the operating phase of the BCI. As can be seen in Table 5, the average classification accuracy for all cases of using various

features in this scenario drops to the chance level again, suggesting that a model that is trained on the data obtained in the presence of pain, will not be a suitable one in the absence of the pain.

Table 5. Classification accuracy results (%) for scenario 4

Features	Scenario 4		
	All	PF	Motor
Max PSD	50.63±2.6	53.75±2.2	50.92±2.4
Med PSD	50.54±2.5	54.05±2.4	50.57±2.3
Var PSD	50.72±2.7	50.78±2.6	50.95±2.6
Max Real{ <i>DFT</i> }	53±2.3	53.52±2.5	51.60±2.7
Freq of Max Real{ <i>DFT</i> }	50.52±2.3	50.69±2.2	50.13±2.5
Freq of Max PSD	50.85±2.4	49.22±2.4	50.47±2.4

In addition, we investigated the question of how the classification accuracy results change if instead of considering all 50 channels, channels from only the motor cortex or from only the prefrontal (PF) cortex are considered. The accuracy results for all four scenarios are shown in Tables 2-5. It can be seen that for scenarios 1 and 3, the use of data from all channels results in an improved accuracy of 1% to 4% compared to using data from the motor channels alone. The improvement in the classification accuracy while using data from all channels ranged from 13% to 20% compared to using data from the prefrontal channels alone. Thus, the classification accuracy is enhanced when data from all channels are used collectively.

V. CONCLUSIONS

In this work, the use of frequency-domain features for classifying mental arithmetic tasks for fNIRS-based BCIs in the absence and the presence of pain was explored. The performance of the classifier model was investigated under four scenarios: 1) the model was trained and tested using pain-free data, 2) the model was trained using pain-free data and tested using under-pain data, 3) the model was trained and tested using under-pain data, and 4) the model was trained using under-pain data and tested using pain-free data. The classification accuracy of the model was taken as the measure of performance. Results indicated that the presence of pain significantly affects the classification accuracy of the model due to its impact on cortical activity.

It was also established that while frequency-domain features of fNIRS signals provide high accuracy results for the classification of the mental arithmetic tasks, they cannot yield a model that is immune to the sudden occurrences of pain. Thus, it is essential to consider the presence of pain in developing BCIs for assistive devices for patients. Additionally, our results indicated that features extracted from both the prefrontal and motor cortices of the brain collectively yield more accurate results as opposed to using features extracted from these areas individually.

Future work will involve exploring features in other domains to identify a set of features that are immune to the presence of pain.

ACKNOWLEDGMENTS

This material is based upon work supported by the National Science Foundation under Grant No. 1841087. Any opinions, findings, and conclusions or recommendations expressed in this material are those of the author(s) and do not necessarily reflect the views of the National Science Foundation.

REFERENCES

- [1] Y. Ardeshipour, A. H. Gandjbakhche, and L. Najafzadeh, "Biophotonics techniques for structural and functional imaging, in vivo," *Stud Health Technol Inform*, vol. 185, pp. 265–97, 2013.
- [2] F. Shamsi, A. Haddad, and L. Najafzadeh, "Early classification of motor tasks using dynamic functional connectivity graphs from EEG," *Journal of Neural Engineering*, vol. 18, no. 1, 2021.
- [3] J. Hennrich, C. Herff, D. Heger, and T. Schultz, "Investigating deep learning for fNIRS based BCI," *37th Annual international conference of the IEEE Engineering in Medicine and Biology Society (EMBC)*, 2015, pp. 2844–2847.
- [4] S. B. Erdoğan, E. Özsarfati, B. Dilek, K. S. Kadak, L. Hanoğlu, and A. Akın, "Classification of motor imagery and execution signals with population-level feature sets: implications for probe design in fNIRS based BCI," *Journal of Neural Engineering*, vol. 16, no. 2, 2019.
- [5] S. B. Borgheai, J. McLinden, A. H. Zisk, S. I. Hosni, R. J. Deligani, M. Abtahi, K. Mankodiya, and Y. Shahriari, "Enhancing communication for people in late-stage ALS using an fNIRS-based BCI system," *IEEE Transactions on Neural Systems and Rehabilitation Engineering*, vol. 28, no. 5, pp. 1198–1207, 2020.
- [6] M. Rea, M. Rana, N. Lugato, P. Terekhin, L. Gizzi, D. Brötzer, A. Fallgatter, N. Birbaumer, R. Sitaram, and A. Caria, "Lower limb movement preparation in chronic stroke: a pilot study toward an fNIRS-BCI for gait rehabilitation," *Neurorehabilitation and Neural Repair*, vol. 28, no. 6, pp. 564–575, 2014.
- [7] M. Peifer, L. Zhu, and L. Najafzadeh, "Real-time classification of actual vs imagery finger tapping using fNIRS," in *Biomedical Optics, OSA Technical Digest*, Optical Society of America, paper BM3A-34, 2014.
- [8] F. Shamsi and L. Najafzadeh, "Multi-class classification of motor execution tasks using fNIRS," *IEEE Signal Processing in Medicine and Biology Symposium (SPMB)*, 2019, pp. 1–5.
- [9] F. Shamsi and L. Najafzadeh, "Multi-class fNIRS Classification of Motor Execution Tasks with Application to Brain-Computer Interfaces," *Biomedical Signal Processing*. Springer, 2021, pp. 1–32.
- [10] A. Comaniciu and L. Najafzadeh, "Enabling communication for locked-in syndrome patients using deep learning and an emoji-based brain computer interface," *IEEE Biomedical Circuits and Systems Conference (BioCAS)*, 2018, pp. 1–4.
- [11] D. A. Seminowicz and M. Moayedi, "The dorsolateral prefrontal cortex in acute and chronic pain," *The Journal of Pain*, vol. 18, no. 9, pp. 1027–1035, 2017.
- [12] R. F. Rojas, X. Huang, J. Romero, and K.-L. Ou, "fNIRS approach to pain assessment for non-verbal patients," *International Conference on Neural Information Processing*, 2017, pp. 778–787.

- [13] R. F. Rojas, X. Huang, and K.-L. Ou, "A machine learning approach for the identification of a biomarker of human pain using fNIRS," *Scientific Reports*, vol. 9, no. 1, pp. 1–12, 2019.
- [14] J. E. Brown, N. Chatterjee, J. Younger, and S. Mackey, "Towards a physiology-based measure of pain: patterns of human brain activity distinguish painful from non-painful thermal stimulation," *PLoS ONE*, vol. 6, no. 9, p. e24124, 2011.
- [15] D. Lopez-Martinez, K. Peng, A. Lee, D. Borsook, and R. Picard, "Pain detection with fNIRS-measured brain signals: a personalized machine learning approach using the wavelet transform and Bayesian hierarchical modeling with Dirichlet process priors," *8th International Conference on Affective Computing and Intelligent Interaction Workshops and Demos (ACIIW)*, 2019, pp. 304–309.
- [16] R. F. Rojas, J. Romero, J. Lopez-Aparicio, and K.-L. Ou, "Pain assessment based on fnirs using bi-1stm rnns," *2021 10th International IEEE/EMBS Conference on Neural Engineering (NER)*, 2021, pp. 399–402.
- [17] F. Shamsi and L. Najafizadeh, "On the effects of pain on fNIRS classification," in *Optics and the Brain, OSA Technical Digest*, Optical Society of America, paper BM4C-6, 2020.
- [18] F. Shamsi, A. Haddad, and L. Najafizadeh, "Recognizing pain in motor imagery EEG recordings using dynamic functional connectivity graphs," *42nd Annual International Conference of the IEEE Engineering in Medicine and Biology Society (EMBC)*, 2020, pp. 2869–2872.